J. Fluid Mech. (1975), *vol.* 68, *part* 2, *pp.* 369–388
Printed in Great Britain

Multiple solutions for flow between coaxial disks

By N. D. NGUYEN, J. P. RIBAULT AND P. FLORENT

Laboratoire de Mécanique des Fluides, Université Laval, Québec, Canada

(Received 10 September 1973 and in revised form 12 August 1974)

The problem of obtaining a numerical solution for the steady flow between two coaxial infinite disks, one fixed and porous, the other rotating, is reduced by von Kármán's hypothesis to solution of a system of nonlinear equations. A Newton-type iteration results in several solutions to these equations, as a number of authors have already indicated. Nevertheless, an interval in which only one solution is found exists for small values of the Reynolds number based on the angular velocity of the rotating disk, the distance between the disks and the kinematic viscosity of the fluid. At large values of this Reynolds number, two solutions appear and have been the subject of intense controversy.

In this paper, both physical and numerical arguments are presented which support a Batchelor-type solution for the flow between infinite disks, in which part of the fluid rotates as a solid body. The other solution, following Stewartson, assumes that the velocity of the fluid outside the boundary layers is entirely axial. This only seems to be verified experimentally when the distance between the disks is large compared with the (finite) radius of the disks.

1. Introduction

Because of its theoretical and practical interest, the problem of laminar flow between two parallel disks has been treated, under unsteady as well as steady boundary conditions, in numerous articles, of which a certain number are cited in the references. Nevertheless, analyses of the problem based upon numerical methods are often contradictory, at least in the case of flow at high Reynolds number. Batchelor (1951) and Stewartson (1953) made different postulates about the nature of the flow which coincide, respectively, in certain regions with those considered by von Kármán (1921) and Bödewadt (1940), who calculated two particular solutions representing flow in the presence of a single disk. The present authors, in a previous treatment of the unsteady flow between coaxial disks, indicated that the solutions in the steady case may be multiple in character in agreement with those found by Mellor, Chappel & Stokes (1968). Greenspan (1972) cast doubt on this character and on the numerical integrity of the solutions by these latter authors and by Rogers & Lance (1962) and Pearson (1965*b*).

We shall limit ourselves here to the case of laminar steady flow between a disk turning with an arbitrary angular velocity Ω_0 and a fixed disk, parallel to the

first, through which uniformly distributed suction or blowing is possible. In comparison with the results presented by different authors, the influence of the parameters controlling the numerical solution of the problem is analysed and, in particular, the question of the initial conditions which must be imposed upon the flow variables is discussed.

The numerical method used is the iterative procedure of Newton. The results are compared with those deduced from the algorithm of Greenspan (1972) and the Runge–Kutta method. Use is made of the results obtained by letting the time T tend towards infinity in the unsteady case treated by Pearson (1965*b*) and Florent, Nguyen & Vo (1973).

Regions in which a unique numerical solution exists are defined as functions of the suction or blowing at the surface of the fixed disk. Other regions are found in which multiple solutions are identified, of which two are *a priori* physically possible. The first corresponds to a flow field with the fluid turning *en bloc* in a zone lying between the boundary layers developing near the disks. This was noted by Batchelor (1951) and in this paper it will be called the Batchelor-type solution. The second corresponds to the configuration postulated by Stewartson (1953), in which the velocity outside the boundary layers has only an axial component. This is the Stewartson-type solution. In the case of no flow through the fixed disk, only the Batchelor type of solution has been confirmed experimentally.

2. Equations of motion and quest for a solution

We shall briefly review the establishment of the equations of the problem. Let us consider two coaxial disks of infinite radius lying in the planes $\bar{z} = 0$ and $\bar{z} = a$. The former disk, through which uniform blowing or suction (of velocity W_0) may be applied, is stationary. The latter is rotating with a constant angular velocity Ω_0. The kinematic viscosity and density of the fluid are respectively ν and ρ. The flow is assumed to be laminar and incompressible.

By symmetry, the problem is described by the Navier–Stokes equations written in cylindrical co-ordinates. As for the unsteady case treated by Florent *et al.* (1973) it is convenient to choose the distance a between the disks as the reference length and ν/a as the reference velocity. The dimensionless radial, tangential and axial velocity components are u, v and w, whilst r and z are the radial and axial co-ordinates normalized with respect to a. Taking also $\rho\nu^2/a^2$ as the reference pressure, we obtain the Navier–Stokes equations in the following form:

$$u\frac{\partial u}{\partial r}+w\frac{\partial u}{\partial z}-\frac{v^2}{r}=-\frac{\partial p}{\partial r}+\frac{\partial}{\partial r}\left(\frac{\partial u}{\partial r}+\frac{u}{r}\right)+\frac{\partial^2 u}{\partial z^2},$$

$$u\frac{\partial v}{\partial r}+w\frac{\partial v}{\partial z}+\frac{uv}{r}=\frac{\partial}{\partial r}\left(\frac{\partial v}{\partial r}+\frac{v}{r}\right)+\frac{\partial^2 v}{\partial z^2},$$

$$u\frac{\partial w}{\partial r}+w\frac{\partial w}{\partial z}=-\frac{\partial p}{\partial z}+\frac{\partial^2 w}{\partial r^2}+\frac{\partial w}{r\,\partial r}+\frac{\partial^2 w}{\partial z^2},$$

$$\partial(ru)/\partial r+\partial(rw)/\partial z=0.$$

The boundary conditions are

$$u = 0, \quad v = 0, \quad w = W_0 a/\nu \quad \text{at} \quad z = 0,$$
$$u = 0, \quad v = ra^2\Omega_0/\nu, \quad w = 0 \quad \text{at} \quad z = 1.$$

With the reference quantities chosen, we obtain a blowing Reynolds number $R_s = W_0 a/\nu$ and a rotation Reynolds number $R_r = \Omega_0 a^2/\nu$, relating the rotation and the distance between the disks.

In order to reduce the number of spatial variables to one, we shall adopt the hypothesis of von Kármán, that the axial velocity is independent of the radial co-ordinate, i.e. $w = f(z)$. It follows from the equation of continuity and the transverse momentum equation that

$$u = -\tfrac{1}{2}rf'(z), \quad v = rg(z).$$

Substituting these expressions for u, v and w into the Navier–Stokes equations and eliminating the pressure by differentiating the first and third equations with respect to z and r respectively, one finds that the unknown functions $f(z)$ and $g(z)$ must satisfy the system

$$\left.\begin{aligned} f^{\mathrm{iv}} - ff''' - 4gg' &= 0, \\ fg' - f'g - g'' &= 0, \end{aligned}\right\} \quad 0 \leqslant z \leqslant 1, \tag{1a}$$

with the boundary conditions

$$\left.\begin{aligned} f(0) = R_s, \quad f'(0) = 0, \quad g(0) = 0, \\ f(1) = 0, \quad f'(1) = 0, \quad g(1) = R_r. \end{aligned}\right\} \tag{1b}$$

For very small Reynolds numbers, analytical solutions exist in the form of double series in terms of the Reynolds numbers, the limiting form being described by Florent & Nguyen (1971). Over other Reynolds number ranges, particularly for high values of R_r, it is necessary to go to a numerical solution.

With f and g known, the pressure distribution can be calculated. Using the momentum equations one obtains

$$p = \tfrac{1}{2}r^2\phi(z) + \psi(z). \tag{2}$$

The new unknown functions ϕ and ψ which define the pressure are given by

$$2\phi + \tfrac{1}{2}f'^2 - ff'' + f''' - 2g^2 = 0,$$
$$\psi + \tfrac{1}{2}f^2 - f' = 0, \quad \phi' = 0.$$

It follows that ϕ is a constant in the steady-state case and can easily be determined using the boundary conditions at $z = 0$ or $z = 1$.

3. Numerical method

Numerical solutions of the differential system (1 *a*) with boundary conditions (1 *b*) have been given by several authors cited in the references. The most widely used numerical procedure is the Runge–Kutta method. This requires imposing three starting values, of $g'(0)$, $f''(0)$ and $f'''(0)$. Recently Greenspan (1972) has

proposed a new algorithm which, according to the author, leads to a rapid olution with a convenient choice of numerical parameters.

Before its use, let us first recall the main points of the iterative method of Newton. This consists of numerically calculating the values F_j and G_j of the functions $f(z)$ and $g(z)$ satisfying the system (1) at the point $z = z_j$. The z interval $[0, 1]$ is divided into n equal parts $\Delta z = 1/n$, such that $z_j = (j-2)\Delta z$. Writing the terms of the system (1) in finite-difference form, and denoting the first and second equations respectively by $\chi_{1,j}$ and $\chi_{2,j}$, one obtains the following system:

$$\left.\begin{aligned}
\chi_{1,j} &= (\Delta z)^{-4}(F_{j-2}-4F_{j-1}-6F_j-4F_{j+1}-F_{j+2}) \\
&\quad +\frac{F_j}{2(\Delta z)^3}(F_{j-2}-2F_{j-1}-2F_{j+1}-F_{j+2})+\frac{G_j}{\Delta z}(G_{j-1}-G_{j+1}), \\
\chi_{2,j} &= (F_j/2\Delta z)\,(G_{j+1}-G_{j-1}) \\
&\quad +\frac{G_j}{12\Delta z}(F_{j+2}-8F_{j+1}+8F_{j-1}-F_{j-2}) \\
&\quad +\frac{1}{(\Delta z)^2}(2G_j-G_{j-1}+G_{j+1})
\end{aligned}\right\} \tag{3}$$

for $$3 \leqslant j \leqslant n+1.$$

The use of central differences in the implicit scheme above assures a satisfactory accuracy, but necessitates the introduction of two supplementary points on the sides: $z_1 = -\Delta z$ and $z_{n+3} = 1+\Delta z$. The values F_1 and F_{n+3} at these points are deduced from the boundary conditions (1 *b*), which can be written as

$$\left.\begin{aligned}
F_2 = R_s, \quad G_2 = 0, \quad F_1 = F_3, \\
F_{n+2} = 0, \quad G_{n+2} = R_r, \quad F_{n+3} = F_{n+1}.
\end{aligned}\right\} \tag{4}$$

We note that the values of $g(z)$ at z_1 and z_{n+3} do not appear in the system (3). This system and (4) together furnish $2(n-1)$ nonlinear equations. We can consider the $2(n-1)$ functions $\chi_{1,j}$ and $\chi_{2,j}$ as functions of the $2(n-1)$ variables $F_3, F_4, \ldots, F_{n+1}$ and $G_3, G_4, \ldots, G_{n+1}$. To start the iterative procedure, we prescribe first approximations F_j and G_j to the solution of (3), and suppose that the differences ΔF_j and ΔG_j from the exact solution $\{\bar{F}_3, \bar{F}_4, \ldots, \bar{F}_{n+1}, \bar{G}_3, , \ldots, \bar{G}_{n+1}\}$ can be calculated from

$$\bar{F}_j = F_j+\Delta F_j, \quad \bar{G}_j = G_j+\Delta G_j \quad \text{for} \quad 3 \leqslant j \leqslant n+1. \tag{5}$$

Developing $\chi_{1,j}$ and $\chi_{2,j}$ as Taylor series and neglecting partial derivatives of order greater than one, the differences ΔF_j and ΔG_j are approximated by the following linear system written in matrix form:

$$\mathbf{D}\begin{bmatrix} \Delta F_3 \\ \vdots \\ \Delta F_{n+1} \\ \Delta G_3 \\ \vdots \\ \Delta G_{n+1} \end{bmatrix} + \begin{bmatrix} \chi_{1,3} \\ \vdots \\ \chi_{1,n+1} \\ \chi_{2,3} \\ \vdots \\ \chi_{2,n+1} \end{bmatrix} = 0,$$

where $$\mathbf{D} = \begin{bmatrix} \frac{\partial \chi_{1,3}}{\partial F_3} & \frac{\partial \chi_{1,3}}{\partial F_4} \cdots \frac{\partial \chi_{1,3}}{\partial F_{n+1}} & \frac{\partial \chi_{1,3}}{\partial G_3} \cdots \frac{\partial \chi_{1,3}}{\partial G_{n+1}} \\ \vdots & & \vdots \\ \frac{\partial \chi_{1,n+1}}{\partial F_3} & & \frac{\partial \chi_{1,n+1}}{\partial G_{n+1}} \\ \frac{\partial \chi_{2,3}}{\partial F_3} & & \frac{\partial \chi_{2,3}}{\partial G_{n+1}} \\ \vdots & & \vdots \\ \frac{\partial \chi_{2,n+1}}{\partial F_3} \cdots & & \cdots \frac{\partial \chi_{2,n+1}}{\partial G_{n+1}} \end{bmatrix}.$$

The new values calculated from (5) will then provide a better approximation to the solution. Using these new values the procedure is repeated until the absolute values of all the functions $\chi_{1,j}$ and $\chi_{2,j}$ become less than some prescribed positive number ϵ.

The calculations were carried out using an IBM-370-155 computer.

4. Discussion of the numerical results without blowing

We shall in turn consider the influence of the choice of the parameters ϵ and Δz and the starting values imposed on the functions f and g on the accuracy and form of the solutions.

Let us recall that a Batchelor-type solution is one where the fluid outside the boundary layers developing over the disks rotates like a solid. In the case of the Stewartson-type solution, the flow is purely in the axial direction outside the boundary layer.

In the following numerical calculations we have taken $|\epsilon| \leqslant 0{\cdot}5$. However, in order to check the accuracy of the results, we also carried out the calculations for a few typical cases with $|\epsilon| \leqslant 0{\cdot}05$. The results differed by at most $10^{-4}\%$, even for a case like $R_r = 1000$, where the velocity gradients are very important.

On the other hand the initial values chosen for f and g have a great influence on both the speed of convergence and the form of the final solution. In the following figures initial values leading to Batchelor-type, Stewartson-type or divergent solutions are denoted respectively by the letters B, S and D.

Let us first consider the case where initially f is taken as zero and g takes any form satisfying the boundary conditions. For $R_r = 500$ (figure 1) it was found that for certain starting values of g the iteration diverges, whilst for others only two distinct solutions exist, at least for the very wide range of values of g chosen. One of these solutions is of Batchelor type, the other of Stewartson type, and they are identical with those obtained by these authors with an appropriate change of co-ordinates. Criteria for the change from one solution to another would seem to be very complicated (figure 1). In fact, in addition to the rotation Reynolds number, the final solution depends on the starting form of $g(z)$ as well as $g'(0)$ and $g'(1)$. Similar results were obtained for the case $R_r = 1000$ (figure 2). One notes that, as in the case $R_r = 500$ (figure 1), an initial linear variation of g (with $f \equiv 0$)

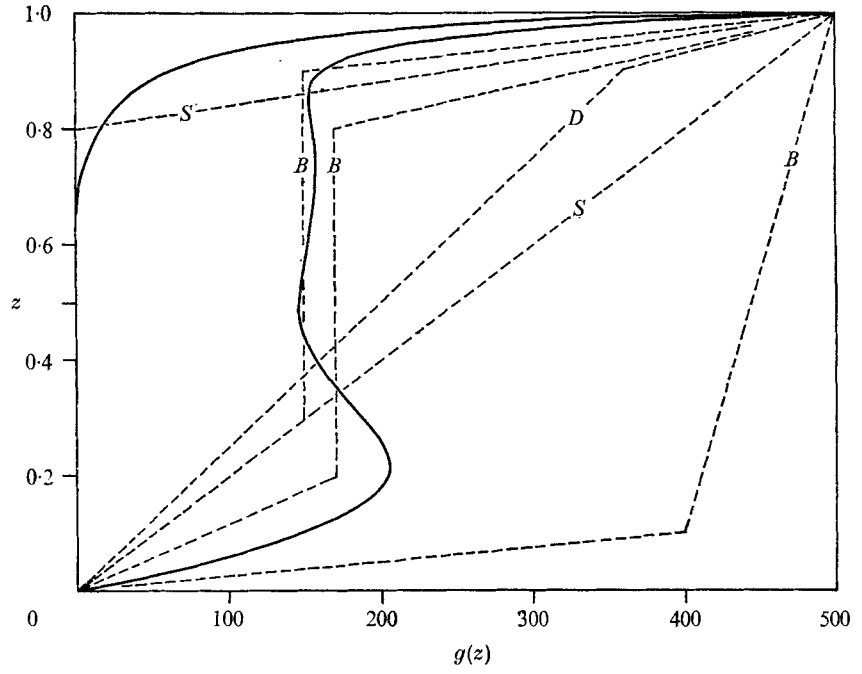

FIGURE 1. ----, starting values for g with $f \equiv 0$; ——, final solutions from steady solution and from time-dependent solution when $T \to \infty$. $R_r = 500$, $R_s = 0$.

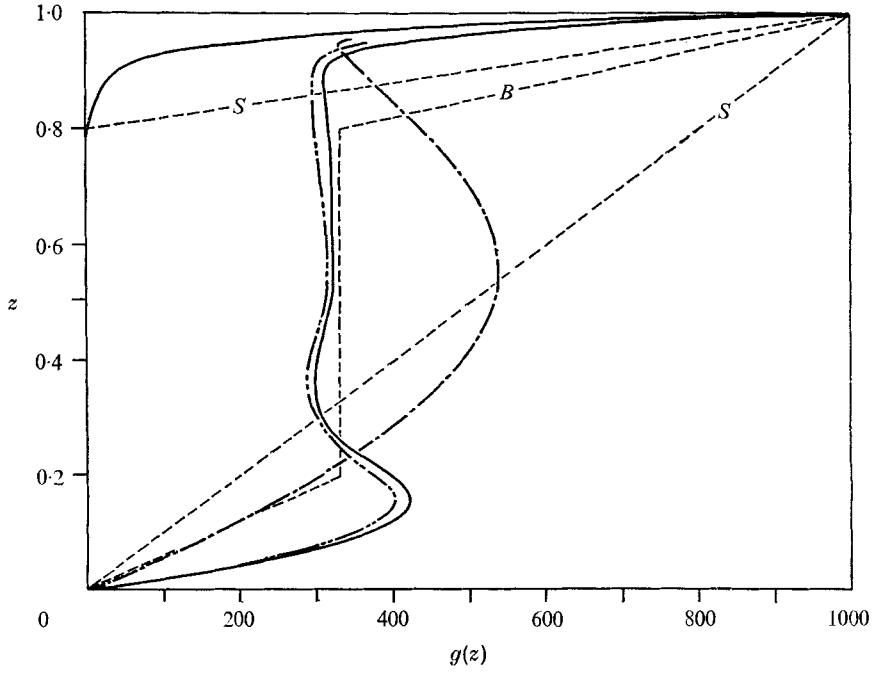

FIGURE 2. ----, starting values for g with $f \equiv 0$; ——, our final solutions, $\Delta z = 0{\cdot}05$; —·—, Greenspan (1972); —··—, Pearson (1965). $R_r = 1000$, $R_s = 0$.

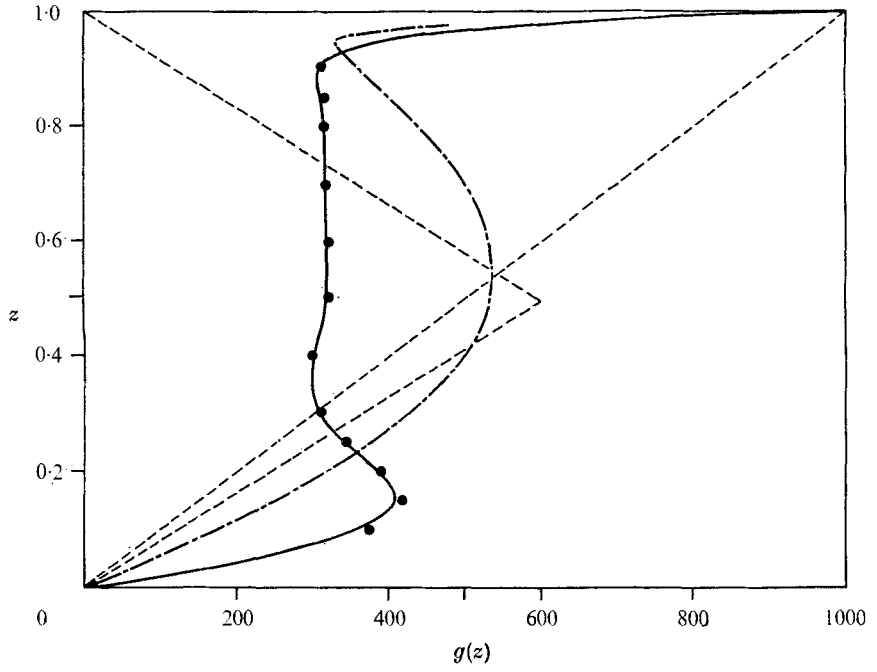

FIGURE 3. Influence of Δz on numerical results. – – –, starting values for f and g; ——, our final solution, $\Delta z = 0{\cdot}02$; ●, our final solution, $\Delta z = 0{\cdot}05$; —·—, Greenspan (1972). $R_r = 1000$, $R_s = 0$.

results in a Stewartson-type solution, which is in disagreement with the results deduced from the unsteady calculation. However if one imposes a triangular form on f (figure 3), analogous to that given by Greenspan (1972), with g linear, one finds, to within $10^{-4}\%$, the Batchelor-type solution already obtained using different starting conditions. Here we can see the importance of the algorithm, which could easily define paths to different solutions from the same initial assumptions. On the other hand, the results given by Pearson (1965*b*) for an unsteady flow set in motion by an impulse correspond approximately to our Batchelor-type solution (figure 2). If we take our results for the unsteady case $R_r(T) = 1000(1 - e^{-9T})$, where $T \to \infty$,† as initial conditions on f and g, we obtain agreement to within $10^{-4}\%$ with our steady-state solution of Batchelor type. This solution, as will be seen later, is experimentally confirmed.

We have chosen $\Delta z = 0{\cdot}05$ ($n = 20$) for almost all the calculations presented here. With $\Delta z = 0{\cdot}02$ or $0{\cdot}05$ in the case $R_s = 0$, $R_r = 1000$, we found the same results for g (figure 3). But we note that, if we take $\Delta z = 0{\cdot}1$, the solution can differ completely from the case $\Delta z = 0{\cdot}05$, although it is still of one of the two types already found. For example, for $R_s = 0$ and $R_r = 400$, we obtained Batchelor- and Stewartson-type solutions by taking $\Delta z = 0{\cdot}05$ and $0{\cdot}1$, respectively, with g linear and $f \equiv 0$ initially. For higher Reynolds numbers ($R_s = 0$, $R_r = 1000$) no solutions were found with $\Delta z = 0{\cdot}1$, which is not surprising in view

† T is considered as infinite when the final value of R_r is within **1** % of the steady-state value *one is aiming to obtain.*

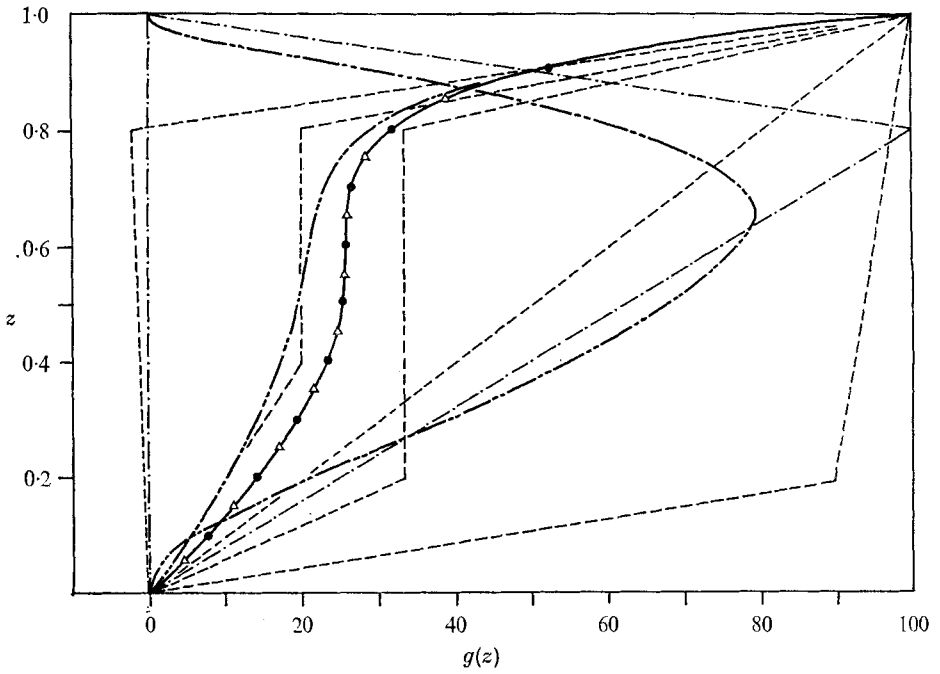

FIGURE 4. ——, final numerical solution; – – –, starting values for f; —·—, starting values for g; —··—, starting values for f and g taken from time-dependent case $R_r(T) = 100 \times (1-e^{-9T})$ at $T = 0{\cdot}6$; Δ, theoretical results from Dorfman (1967); ●, theoretical results from Pearson (1965*b*). $R_r = 100$, $R_s = 0$.

of the large velocity gradients. On the other hand, for smaller Reynolds numbers, the choice of Δz is less important, and even taking $\Delta z = 0{\cdot}1$ will provide a comparable solution, which is almost identical, provided that $R_r \leqslant 50$.

It must also be recalled that the numerical method chosen has an important influence on the nature of the resulting solution. Thus in the test case $R_s = 0$, $R_r = 1000$, the Runge–Kutta method only leads to a Stewartson-type solution, and not to that of Batchelor type, which has only been verified recently, in particular by work on unsteady flows.

However, if the previous results pose the question of the existence of a multiplicity of solutions of the present problem, the numerical results indicate that at lower Reynolds numbers only one solution is possible. For example, for $R_s = 0$ and $R_r = 100$ (figure 4), the solution is the same to within $10^{-4}\%$ for all the initial conditions on f and g mentioned. The Runge–Kutta method provides identical results, consistent with the experimental results of Mellor *et al.* (1968) as well as those of Florent *et al.* (1973).

On the basis of the present numerical results, we shall now define, in terms of the rotation Reynolds number, the regions where one, two or even several solutions exist. The form of the solution is easily specified by the tangential velocity $g(z)$, with $g'(0)$ negligible or not, corresponding to the Stewartson- and Batchelor-type solutions respectively. Figure 5 indicates the existence of three regions delimited by $R_r = 200$ and 300.

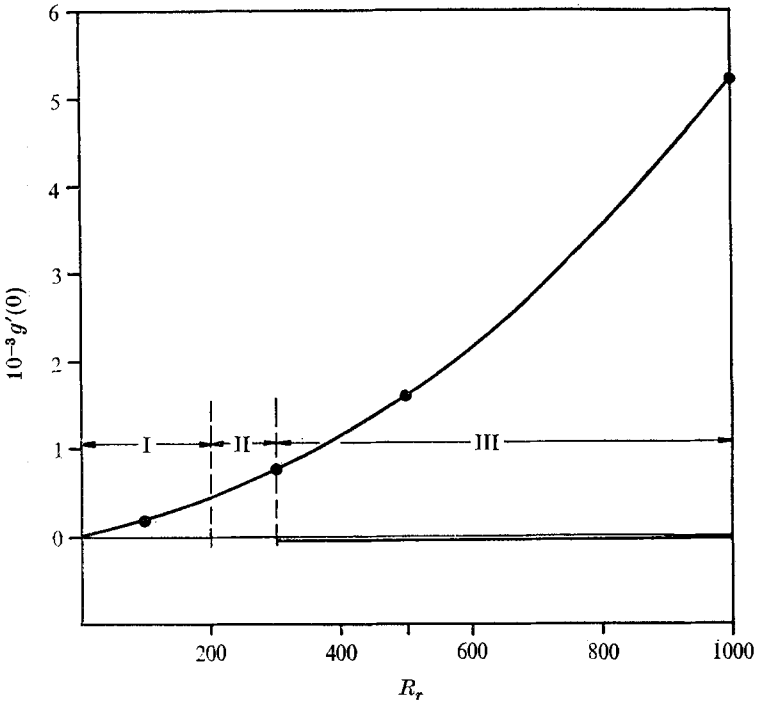

FIGURE 5. ——, theoretical results from steady case; ●, theoretical results from time-dependent case $R_r(T) = R_r(1-e^{-9T})$, when $T \to \infty$, $R_s = 0$.

Region I is where only one solution was found for a wide variety of initial conditions on f and g. In region III, $R_r > 300$, two solutions exist. That of Batchelor type is the only one which is obtained from the solution of the unsteady rotating-disk problem when the motion tends to a steady state as $T \to \infty$. The Stewartson-type solution is only obtained by the Runge–Kutta method and that of Newton with certain initial values of f and g, as previously mentioned. Lastly, region II, $200 < R_r < 300$, is where a Batchelor-type solution is found, with the solution varying continuously from those of region I. What differentiates the two regions is that the initial conditions for the Batchelor-type solution must be chosen very close to the actual solution to ensure convergence in region II.

5. Comparison between experimental and theoretical results without blowing

The installation contains two disks 30 cm in diameter. The speed of the rotating disk can be varied up to 12 000 r.p.m. The distance between the disks is continuously adjustable, whilst still preserving parallelism. This is essential, since any slight asymmetry can considerably change the flow pattern. Static pressures were obtained from holes of diameter 0·2 mm along two perpendicular diameters of the fixed disk. Hot-wire measurements were also carried out using a wall probe whose design was based on a study of the influence of probe supports in strong velocity gradients given by Florent & Thiolet (1969). For comparison purposes

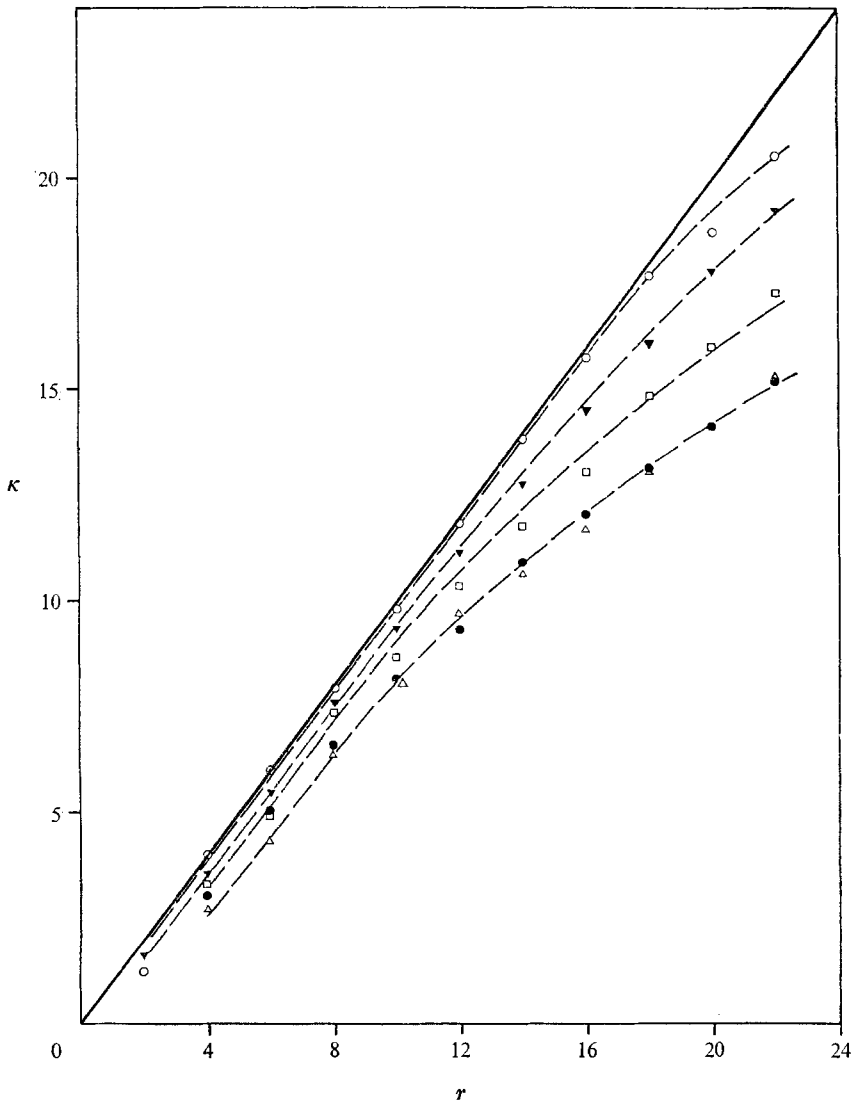

FIGURE 6(*a*). For legend see facing page.

we also used the same probe with the support placed between the disks. The measurements were limited to regions of laminar flow.

We tried to determine the regions where the above theory, based on infinite disks, applies to disks of finite dimensions. This involves finding the limits of the validity of the numerical solution, by checking basic theoretical hypotheses such as the independence of the axial component of velocity of radial distance. To achieve this, a comparison has been made between the pressure gradients measured over the fixed disk, the mean velocity field and the corresponding numerical solutions.

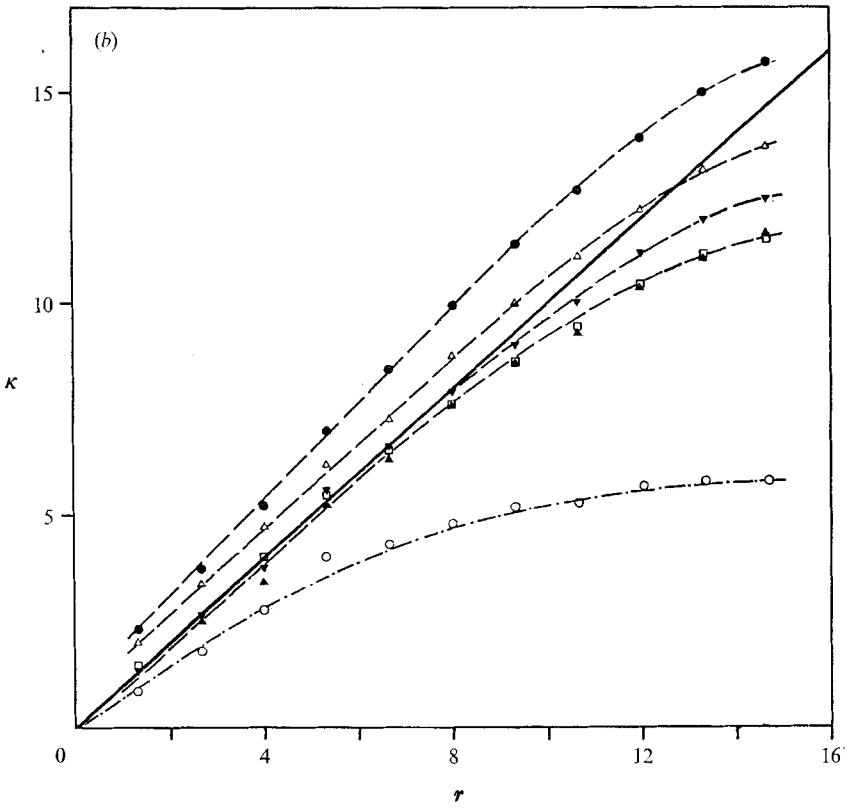

FIGURE 6. Radial pressure distributions on the fixed disk. ——, theoretical curve; – – – –, experimental results from laminar regime; —·—, experimental results from fully turbulent regime. (*a*) $a/R_d = \frac{1}{24}$. (*b*) $a/R_d = \frac{1}{16}$.

	▲	○	▼	□	●	△
(*a*) R_r		1256	942	628	392	308
(*b*) R_r	1256	1256	1884	1570	2512	2198

If $\bar{p}_0$ denotes the pressure at the centre, which for a given fluid depends upon the distance between the disks and the speed of rotation, then from (2)

$$\frac{\bar{p}-\bar{p}_0}{\frac{1}{2}\rho\nu^2/a^2} = \frac{\bar{r}^2}{a^2}\phi, \quad \text{where} \quad \phi = \phi(R_r).$$

For varying Reynolds number, a plot of

$$\left((\bar{p}-\bar{p}_0)/\tfrac{1}{2}\rho\frac{\nu^2}{a^2}\phi_{\text{th}}\right)^{\frac{1}{2}} = \kappa$$

as function of $r = \bar{r}/a$ should consist theoretically of one straight line of unit slope, where ϕ_{th} is the numerical value calculated for ϕ.

From figures 6 (*a*) and (*b*), corresponding to different distances between the disks and speeds of rotation, we note that the Reynolds number R_r provides a good characterization of the problem in an annular region, where the experi-

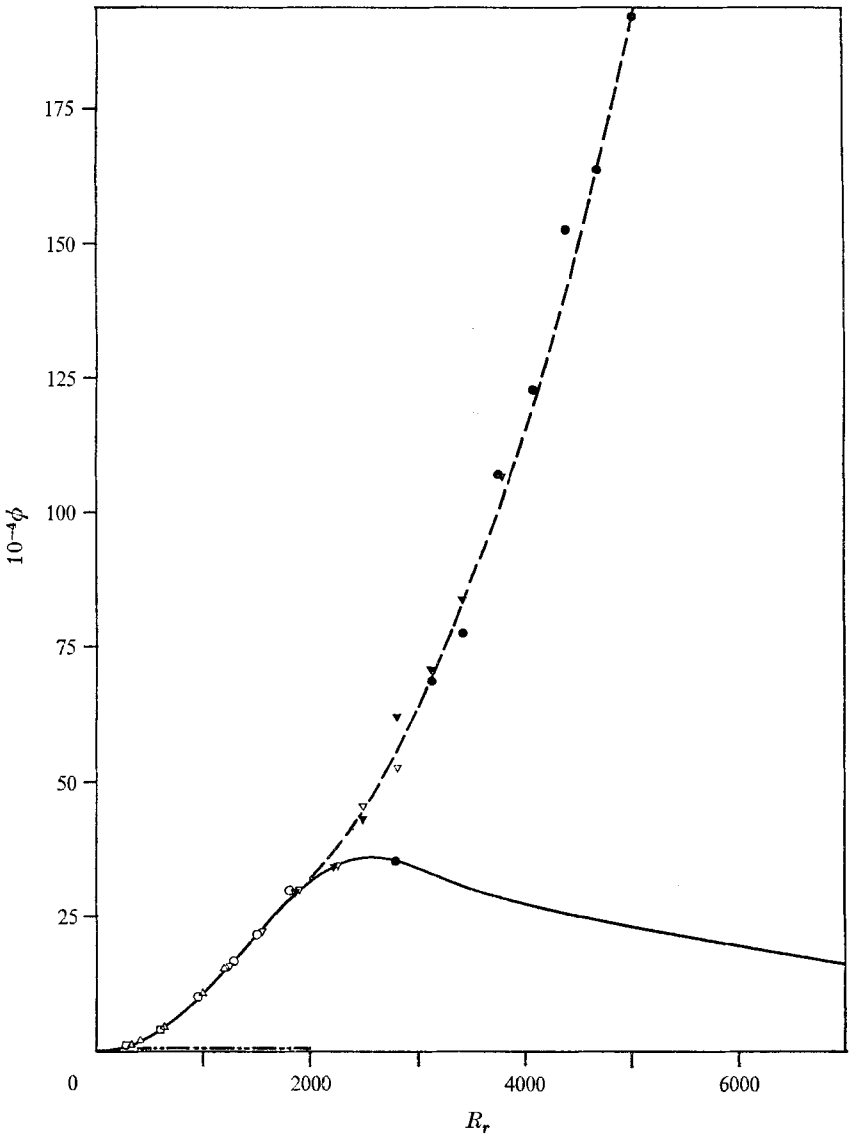

FIGURE 7. Variation of radial pressure gradient with rotating Reynolds number. ——, numerical results, Batchelor-type solution; —·—, numerical results, Stewartson-type solution; – – –, experimental results.

	●	▼	▽	○	△	□
$\frac{a}{R_d}$	$\frac{8}{96}$	$\frac{7}{96}$	$\frac{6}{96}$	$\frac{5}{96}$	$\frac{4}{96}$	$\frac{3}{96}$

mental $\partial^2 p/\partial r^2$ corresponds to that deduced from the theoretical solution. Moreover the assumption that the flow is laminar in this region was also confirmed.

Figure 7 shows that the overall data concerning the function ϕ defining $\partial^2 p/\partial r^2$ are in good agreement with the theory for Reynolds numbers below 2000. Comparison of this evolution of ϕ with those deduced from the velocity fields of

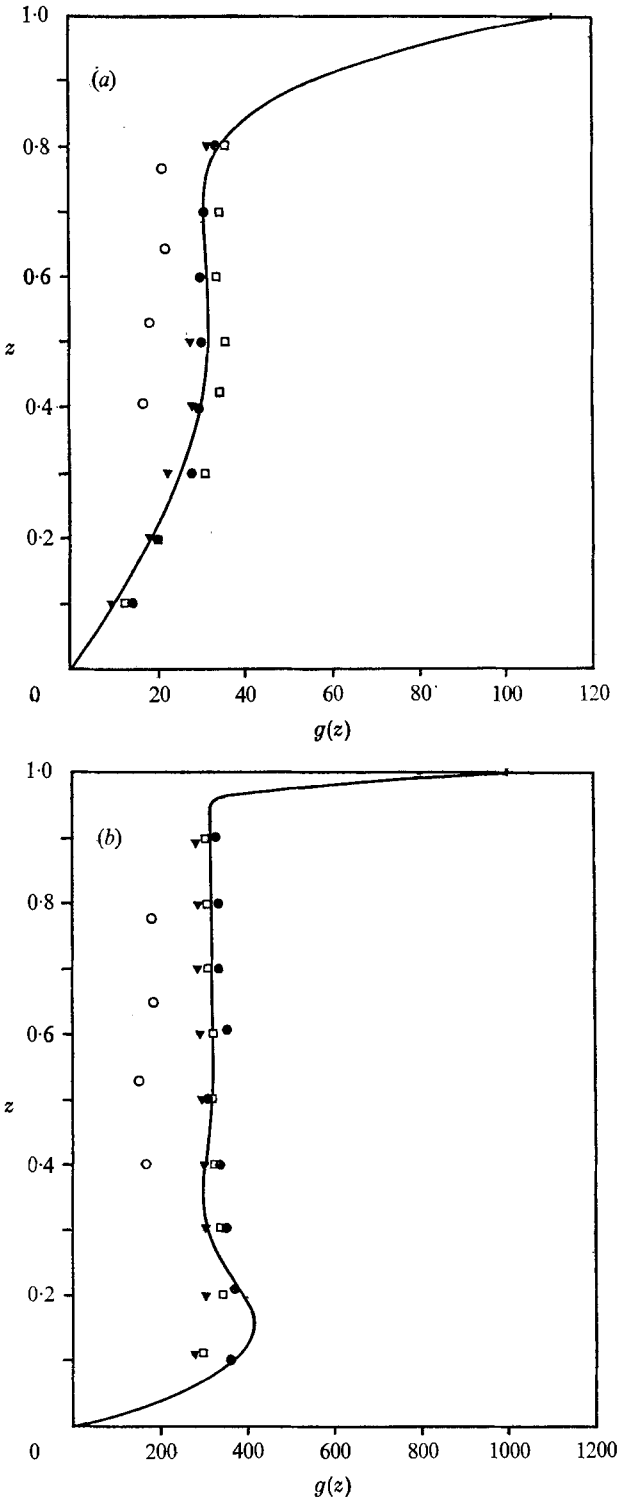

FIGURE 8. Experimental and theoretical results for various Reynolds numbers. ——, theoretical curve; □, $r = 6$; ●, $r = 8$; ▼, $r = 12$; ○, probe with support between disks, $r = 8$. (*a*) $R_r = 110{\cdot}4$. (*b*) $R_r = 993{\cdot}8$.

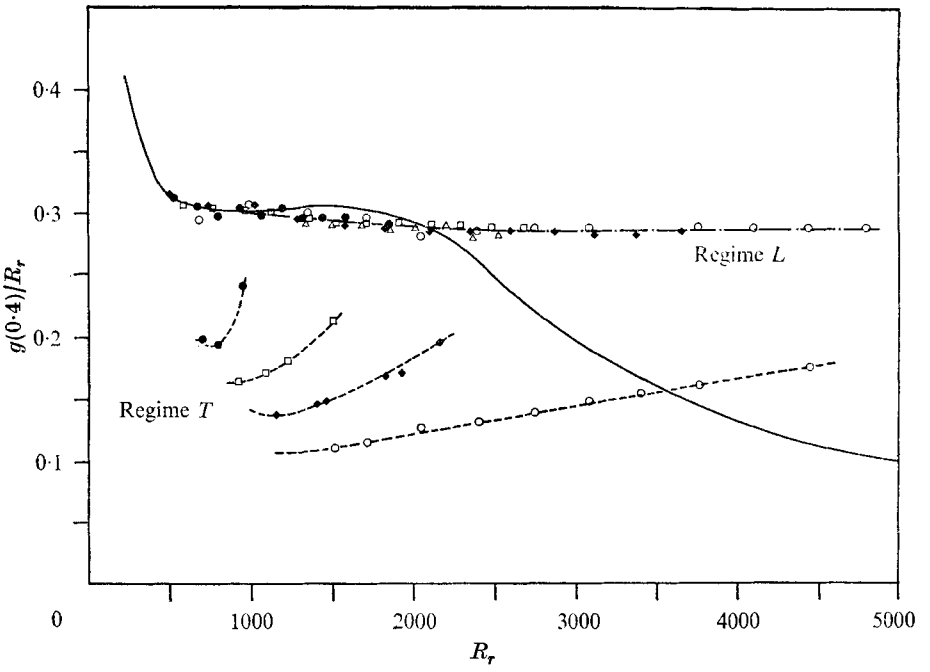

FIGURE 9. Variation of $g(0{\cdot}4)/R_r$ with rotating Reynolds number R_r. ——, theoretical curve, Batchelor-type solution; – – –, experimental results from fully turbulent regime; —·—, experimental results from laminar regime.

	△	●	□	◆	○
$\frac{a}{R_d}$	$\frac{4}{96}$	$\frac{5}{96}$	$\frac{6}{96}$	$\frac{7}{96}$	$\frac{8}{96}$

Batchelor and Stewartson indicates that only the Batchelor-type solution agrees with the experimental data.

Limiting ourselves to the laminar regions, where the experimental and theoretical $\partial^2 p/\partial r^2$ are in agreement, we see from figures 8 (*a*) and (*b*) that the two sets of mean velocity profiles are consistent, and correspond to the Batchelor-type solution. It is important to underline the large differences arising from the particular anemometry techniques used. Only the wall probe provided data consistent with the theory. The same probe with a support in the flow between the disks both slowed down the flow and modified the overall pattern.

The ratio of the rotational speed of the fluid to that of the disk, represented approximately by $g(0{\cdot}4)/R_r$, varied in the same manner as the previous results as regards the limit $R_r < 2000$ (figure 9). For $a/R_d > \frac{5}{96}$ (R_d = radius of disks) two stable experimental flow patterns were observed over a range of Reynolds numbers which increased with the distance between the disks. We shall call these two regimes *T* and *L*.

Regime *T* corresponds to fully developed turbulent flow between the disks. For regime *L* the flow is laminar inside an annular region, and corresponds to an accelerating flow. It will be seen from figure 6 (*b*) that for a given Reynolds number only regime *L* furnishes data for $\partial^2 p/\partial r^2$ in agreement with the theory.

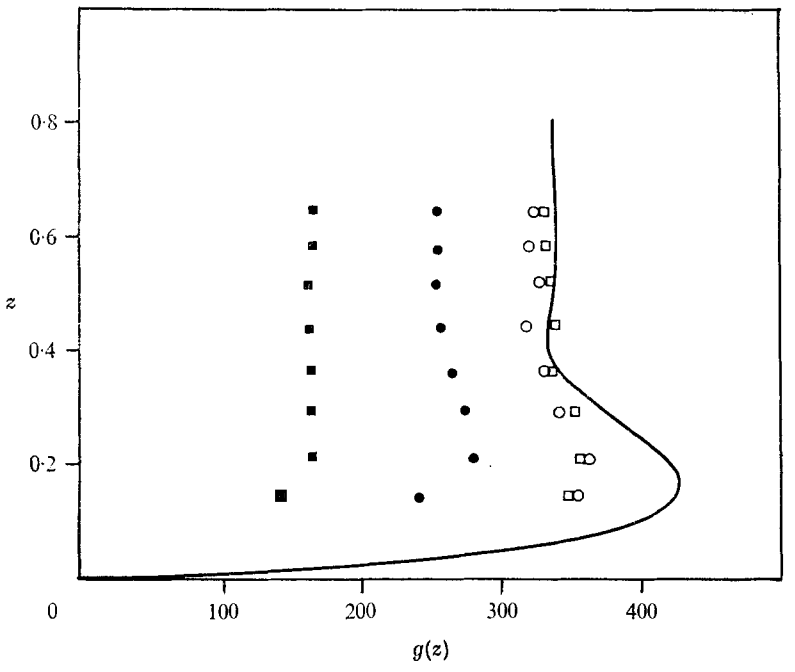

FIGURE 10. Tangential velocity distributions. ——, theoretical curve, Batchelor-type solution; ○, experimental results, $\bar{r}/R_d = \frac{1}{4}$; □, experimental results, $\bar{r}/R_d = \frac{1}{2}$. Open symbols, laminar flow; filled symbols, fully turbulent flow. $a/R_d = \frac{1}{86}$, $R_r = 1100$.

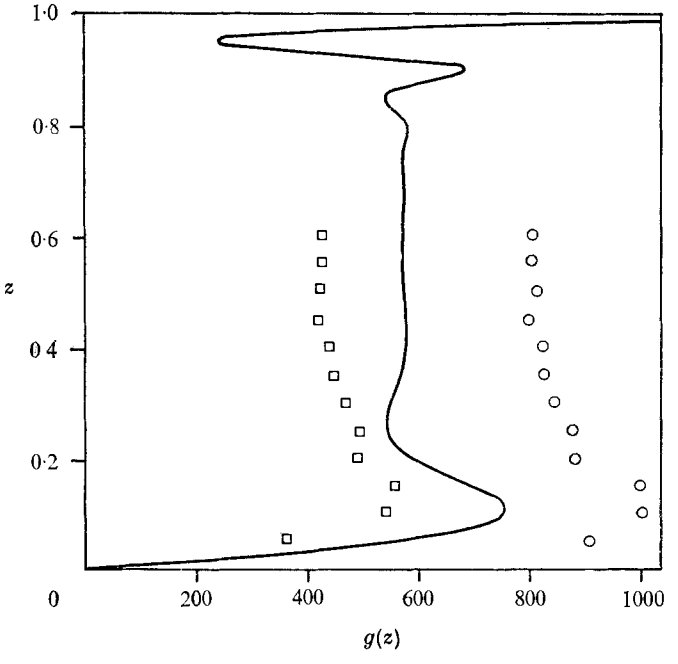

FIGURE 11. Tangential velocity distributions at $\bar{r}/R_d = \frac{1}{3}$. ——, theoretical curve, Batchelor-type solution; □, experimental results corresponding to fully turbulent flow; ○, experimental results corresponding to laminar flow. $a/R_d = \frac{1}{12}$, $R_r = 3135$.

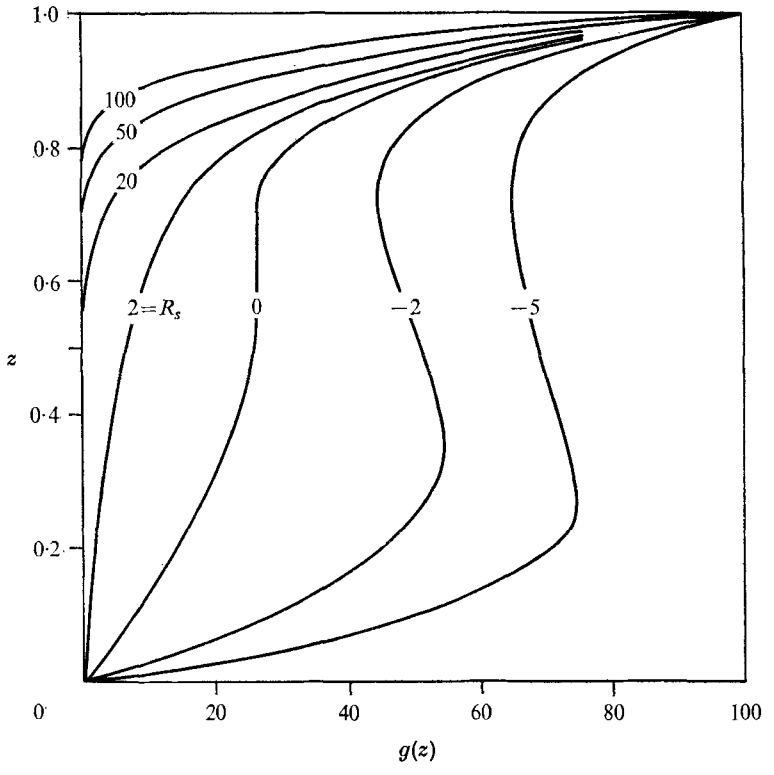

FIGURE 12. Influence of blowing or sucking on the form of theoretical tangential velocity distribution. $R_r = 100$.

The experimental change from T to L occurs automatically at a Reynolds number which increases with the distance between the disks. Below this limit the change from T to L or vice versa can be triggered by a small perturbation.

For $R_r < 2000$ (figure 10), the tangential velocity profiles corresponding to each of these regimes show that good agreement with the numerical calculations is obtained in the laminar configuration, which is characterized by an annular region where similarity exists and where $\partial^2 p/\partial r^2$ remains constant. In the turbulent regime, similarity ceases to exist (figure 10) and $\partial^2 p/\partial r^2$ is never constant (figure 8*b*). For $R_r > 2000$, the agreement fails but the experimental profile still remains of Batchelor type (figure 11).

6. Theoretical influence of sucking or blowing

Figure 12 indicates that the solutions tend to be respectively of the Stewartson and Batchelor types for the cases of blowing and sucking through the fixed disk, which seems physically plausible. In figure 13, one finds three characteristic zones, as in the case $R_s = 0$. The region with a unique numerical solution is larger in the case of blowing than for sucking. However, results deduced from evolution of an unsteady flow ($T \to \infty$) always give the solution corresponding to the largest couple acting on the fixed disk.

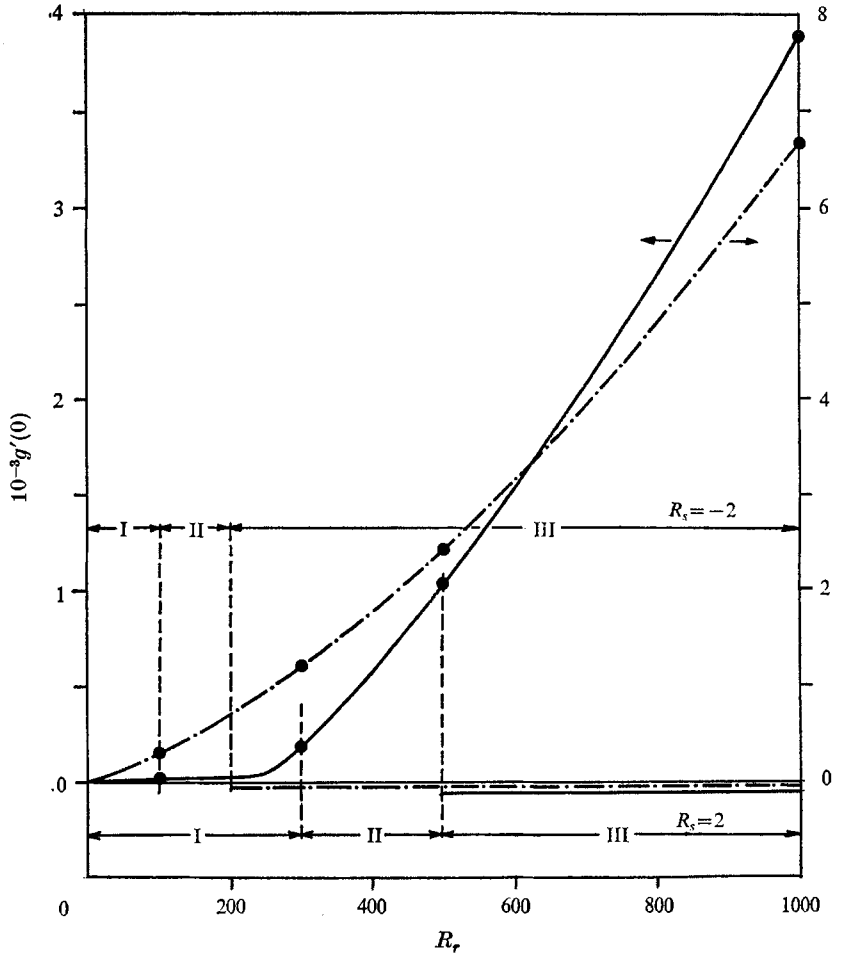

FIGURE 13. Theoretical results. ——, steady case, Batchelor-type solution; —·—, steady case, Stewartson-type solution; ●, time-dependent case, $R_r(T) = R_r(1-e^{\beta T})$ when $T \to \infty$.

7. Discussion

As Rott & Lewellen (1965) have pointed out, the Batchelor-type solution is not a singular solution of the boundary-layer equations. In the light of the previous numerical results, we shall try to justify the validity of one solution, that of Batchelor type.

Our own results, as well as those of Mellor *et al.* (1968) and those of Pearson (1965*b*), which were all obtained using different algorithms, lead us to believe that several solutions exist. Greenspan (1972) asserts the uniqueness of his solution, with strong restrictions on his convergence criteria or 'relaxation parameters'. However, he does seem to have omitted to verify, at least for the case $R_r = 1000$, $R_s = 0$, the dominant influence of the starting values of f and g on the final solution. In fact we have noticed, in particular, that the convergence criterion in our algorithm is much less important than the choice of the starting values of

f and g. For a wide variety of the latter values, only two types of solutions were found, corresponding respectively to those of Batchelor and Stewartson. We cannot of course claim that these are the only solutions, since it is impossible to try all possible initial combinations of f and g. But to our knowledge the algorithm used here is the only one which leads to a solution corresponding to the experimental results, even when the Reynolds number is high.

To summarize, it is not possible with the present state of development of the numerical analysis of the steady case to confirm one or other of the two types of solution. Nevertheless we have certain indications of the uniqueness of the solutions from our results in unsteady radial flows. We have found that, if the rotating disk accelerates from rest to some arbitrary steady state, then the final solution, as time tends to infinity, is always of Batchelor type, independently of the Reynolds number R_r. The results of Pearson (1965*b*), for the case of a rotating disk subjected to an impulse, indicate the same tendency. Also our calculations show that a numerical perturbation of the Stewartson-type solution for $R_r(T) > 3000$, in an unsteady evolution, gives rapidly a Batchelor-type solution.

Figure 5 is also very significant. The value of $g'(0)$ and the couple arising from the tangential friction acting on the fixed disk increase together up to $R_r \sim 200$. Afterwards, $g'(0)$ can either continue to increase monotonically or drop abruptly to virtually zero. The first possibility, corresponding to the Batchelor-type solution, thus seems more plausible, in view of the discontinuity represented by the evolution of the Stewartson-type solution.

From the physical point of view, the two types of solution both seem possible. For a given fluid, a large Reynolds number R_r implies either a large distance between the disks or a high speed of rotation. In the first case, one can eventually envisage a negligible couple acting on the fixed disk, that is to say a Stewartson-type solution. In the second case, the influence of the rotating disk on the stationary one is much greater, which leads us to consider a Batchelor-type solution.

However, this generally accepted reasoning is invalidated by the following two facts. First, it does not explain why only one numerical solution has been found by every author in the case of small Reynolds numbers. Second, it is based on a physical configuration with disks of finite radius. If one imagines infinite disks as postulated in the formulation of the problem, the fluid between the boundary layers would turn like a solid at a speed lower than that of the rotating disk.

The previous assertions are based on experimental observations. In fact, from our measurements between disks 30 cm in diameter, we have noted that the torque acting on the fixed disk is never zero and can be measured as long as the distance between the disks remains less than 5 cm. This couple increases with the speed of rotation. We have further observed that the fluid is in solid rotation in the plane halfway between the disks, and that the theoretical and experimental velocity profiles are the same as long at $R_r < 2000$. For small distances between the disks the results of Schultz–Grunow (1935) confirm this result, as well as our experimental results given in figure 9, and those of Mellor *et al.* (1968), which justify the existence of the Batchelor-type solution. In addition, if the flow develops in the space between two disks and a bounding cylinder attached to the

stationary disk, it has been found by Rogers & Lance (1960), and Maxworthy (1963) that the fluid is in solid rotation. It may be noted that only the Batchelor-type solution is found with this configuration.

8. Conclusion

The numerical resolution of the steady radial flow between a stationary and a rotating disk effectively furnishes several possible solutions. This multiplicity of solutions is probably inherent in the nonlinear character of the system of basic equations, rather than inaccuracies in the numerical procedure. Nevertheless, there exists, for low Reynolds numbers, a region where only one solution seems to occur, which is independent of the numerical method.

At higher Reynolds numbers two numerical solutions were found. We have presented various arguments both from the numerical and the physical point of view favouring one type of solution, that of Batchelor type, in which a part of the fluid between the disks is in solid-body rotation.

On the other hand, with certain restrictions on the distance between the disks and the speed of rotation, two stable solutions have been also observed experimentally. The first one, in disagreement with the numerical results, is a turbulent configuration. In this case, the similarity ($v = rg$) does not exist and $\partial^2 p/\partial r^2$ is never constant. The second, in good agreement with the numerical results for $R_r < 2000$, is characterized by an annular region where similarity exists and where $\partial^2 p/\partial r^2$ remains constant.

The authors would like to thank the National Research Council of Canada for their financial support (Grant A-7924) and Dr E. J. Dickinson of Laval University for valuable discussions.

REFERENCES

BATCHELOR, G. K. 1951 Note on a class of solution of the Navier–Stokes equations representing rotationally symmetric flow. *Quart. J. Mech. Appl. Math.* **4**, 29.

BÖDEWADT, U. T. 1940 Die Drehströmung über festem Grunde. *Z. angew. Math. Mech.* **20**, 241.

COCHRAN, W. G. 1934 The flow due to a rotating disc. *Proc. Camb. Phil. Soc.* **30**, 365.

DORFMAN, L. A. 1967 Flow of a viscous fluid between fixed and blown rotating discs. *N.A.S.A. Tech. Rep.* TTF-10, 931.

FLORENT, P. & NGUYEN, N. D. 1971 Ecoulement instationnaire entre un disque fixe poreux et un disque tournant. *IUTAM Symp. Unsteady Boundary Layers, Laval University, Quebec*, p. 1216.

FLORENT, P., NGUYEN, N. D. & VO, N. D. 1973 Ecoulement instationnaire entre disques coaxiaux. *J. Mécanique*, **12**, 555.

FLORENT, P. & THIOLET, G. 1969 Importance de l'orientation du support de sonde à fil chaud par rapport à une paroi sur la détermination des vitesses moyennes dans une couche limite turbulente. *C. R. Acad. Sci. Paris*, **269**, 405.

GREENSPAN, D. 1972 Numerical studies of flow between rotating coaxial discs. *J. Inst. Math. Appl.* **9**, 370.

GROHNE, D. 1955 Uber die laminare Strömung in einer Kreiszylindrischen Dose mit rotierendem Deckel. *Nachr. Akda. Wiss. Göttingen, Math. Phys.* **1** (II*a*), 263.

KÁRMÁN, T. VON 1921 Laminar und turbulente Reibung. *Z. angew. Math. Mech.* **1**, 233.

MAXWORTHY, T. 1963 The flow between a rotating disc and a coaxial stationary disc. *Space Prog. Summ.* no. 37.27, vol. 4, §327. Jet Propulsion Laboratory, Pasadena, California.

MELLOR, G. L., CHAPPEL, P. J. & STOKES, V. K. 1968 On the flow between a rotating and a stationary disk. *J. Fluid Mech.* **31**, 95.

PEARSON, C. E. 1965*a* A computational method for viscous flow problems. *J. Fluid Mech.* **21**, 611.

PEARSON, C. E. 1965*b* Numerical solutions for the time-dependent viscous flow between rotating coaxial disks. *J. Fluid Mech.* **21**, 623.

PEUBE, J. L. 1967 Ecoulement entre un disque fixe poreux et un disque tournant. *Cong. Can. Mécanique Appl., Québec.*

ROGERS, M. H. & LANCE, G. N. 1960 The rotationally symmetric flow of a viscous fluid in the presence of an infinite rotating disk. *J. Fluid Mech.* **7**, 617.

ROTT, N. & LEWELLEN, W. S. 1965 Examples of boundary layers in rotating flows. *Agardograph*, **97**, 613.

SCHULTZ-GRUNOW, F. 1935 Der Reibungswiderstand rotierender Scheiben in Gehäusen. *Z. angew. Math. Mech.* **15**, 191.

STEWARTSON, K. 1953 On the flow between two rotating coaxial discs. *Proc. Camb. Phil. Soc.* **3**, 333.

STUART, J. T. 1954 On the effects of uniform suction on the steady flow due to a rotating disc. *Quart. J. Mech. Appl. Math.* **7**, 466.